sustainability

MDPI

Article

Proposing a GEE-Based Spatiotemporally Adjusted Value Transfer Method to Assess Land-Use Changes and Their Impacts on Ecosystem Service Values in the Shenyang Metropolitan Area

Shuming Ma [1,*], Jie Huang [1] and Yingying Chai [2]

[1] Key Laboratory of Industrial Ecology and Environmental Engineering (Ministry of Education), School of Environmental Science and Technology, Dalian University of Technology, Dalian 116024, China; jiehuangedu@hotmail.com

[2] Institute of Ecology, Chinese Research Academy of Environmental Sciences, Beijing 100012, China; chai.yingying@craes.org.cn

* Correspondence: shumingma@dlut.edu.cn

Abstract: Understanding land-use dynamics and their impacts on ecosystem service values (ESVs) is critical to conservation and environmental decision-making. This work used the Google Earth Engine (GEE) platform and an adjusted value transfer method to investigate spatiotemporal ESV changes in the Shenyang Metropolitan Area (SMA), a National Reform Pilot Zone in northeast China. First, we obtained land-use classification maps for 2000, 2005, 2010, 2015, and 2020 using a GEE-based Landsat dense stacking methodology. Then, we employed four spatiotemporal correction factors (net primary productivity, fractional vegetation cover, precipitation, and crop yield) in the value transfer method, and analyzed the ESV dynamics. The results showed that forest land and cropland were the two dominant land-use types, jointly occupying 75–89% of the total area. The built-up areas expanded rapidly from 2727 km^2 in 2000 to 3597 km^2 in 2020, while the cropland kept decreasing, and suffered the most area loss (−1305.09 km^2). The ESV of the SMA rose substantially from 814.04 hundred million Chinese Yuan (hmCYN) in 2000 to 1546.82 hmCYN in 2005, then kept decreasing in 2005–2010 (−17.01%) and 2010–2015 (−10.75%), and finally increased to 1329.81 hmCYN in 2020. The ESVs of forest comprised most of the total ESVs, with the percentage ranging from 72.65% to 77.18%, followed by water bodies, ranging from 11.61% to 15.64%. The ESV changes for forest land and water bodies were the main drivers for the total ESV dynamics. Overall, this study illustrated the feasibility of combining the GEE platform and the spatiotemporal adjusted value transfer method into the ESV analysis. Additionally, the results could provide essential references to future environmental management policymaking in the SMA.

Keywords: Google Earth Engine; land use; the Shenyang Metropolitan Area; ecosystem service values

Citation: Ma, S.; Huang, J.; Chai, Y. Proposing a GEE-Based Spatiotemporally Adjusted Value Transfer Method to Assess Land-Use Changes and Their Impacts on Ecosystem Service Values in the Shenyang Metropolitan Area. *Sustainability* **2021**, *13*, 12694. https://doi.org/10.3390/su132212694

Academic Editor: Francesco Caracciolo

Received: 13 October 2021
Accepted: 9 November 2021
Published: 17 November 2021

1. Introduction

Ecosystems provide a wide range of direct or indirect services to human well-being, called ecosystem services [1,2]. The Millennium Ecosystem Assessment classified ecosystem services into four main categories: provisioning services (e.g., food and raw materials), regulating services (e.g., climate regulation and flood regulation), supporting services (e.g., nutrient cycling and soil formation), and cultural services (e.g., recreation and aesthetic appreciation) [1]. These services provide necessary guarantees and support for human existence and good quality of life [3–6], and are recognized as a critical foundation for achieving the United Nations Sustainable Development Goals (SDGs) [6–8]. However, with increasingly intense human activities such as urban development and population growth, the structure and service functions are significantly undermined and degraded

over time and space [9–11]. For example, the Intergovernmental Science-Policy Platform on Biodiversity and Ecosystem Services (IPBES) Global Assessment report noted that human actions had altered 75% of land-based environment, and approximately 66% of the marine environment [12]. The total global ecosystem service values in 2007 were 145 trillion/year and dropped to 125 trillion/year in 2011 [10]. Land-use changes, an essential indicator of human activities, are the main driving forces for altering ecosystem services [1,13,14]. Thus, evaluating land-use dynamics and their impact on ecosystem service values (ESVs) could provide essential information for ecosystem services-based conservation and environmental decision-making [15–17], and has attracted worldwide attention [18,19].

Analyzing ESV changes usually requires two prerequisites: land use data and the ESV assessment method, which links land use with ESVs. One way to obtain land use data is to directly adopt existing databases, which are usually expensive or only available for specific areas and periods. Another way is through remote sensing to process satellite imageries. However, this method involves significant data acquisition and storage tasks, and needs high computing costs, especially for large areas such as on the regional and global scales [20]. Google launched a cloud-based platform named the Google Earth Engine (GEE) [21], which provides free access to more than 40 years' worth of worldwide satellite images at a petabyte-scale. GEE also offers a packaged algorithm for image preprocessing with relative ease, for example, machine learning classifiers for land use classification [22,23]. Overall, GEE provides user-friendly and high-performance geospatial tools to process large data sets for regional and global applications [24], and now has been wildly adopted into various decision-making contexts, such as vegetation mapping [25,26], agricultural productivity assessment [27,28], and land cover mapping [22,23,25,29–31]. As for ESV assessment methods, one of the most well-known is the benefit transfer approach proposed by Costanza et al., which covers 17 ecosystem services for 16 biomes and estimates their equivalent value per unit area globally. This method is intuitive, has fewer data requirements, is particularly suitable for assessing ESVs at the regional and global scales [12,17,32], and, therefore, is widely adopted across the world [9,32–34]. For example, Xie et al. [35,36] built an equivalent coefficient table based on Costanza et al. that has been extensively used in China [7,12,37–39]. However, the value transfer methods are frequently criticized for simply handling the complexity and spatial heterogeneity of the ecosystem by using static and global value factors. Therefore, numerous studies have attempted to introduce biophysical and statistical adjustment factors for spatial and temporal corrections of the value coefficient. For example, Xie et al. adopted net primary productivity (NPP), erosion prevention, and precipitation factors to evaluate the ESV changes in China [32]. Song et al. analyzed the spatial ESV changes in the North China Plain by introducing NPP and soil erosion factors [40]. Sannigrahi et al. used multiple factors, including a normalized difference vegetation index (NDVI), NPP, fractional vegetation cover (FVC), precipitation, and crop yield for ESV evaluation of a natural reserve region [41].

For this study, we combined the advancements in land-use analysis and value transfer methods to investigate ESV changes in the Shenyang Metropolitan Area (SMA). The SMA is a critical National Reform Pilot Zone in northeast China, and has experienced rapid economic development and urbanization processes, resulting in massive environmental pressure in recent decades. However, a significant indicator of human activities—land-use changes—and their effects on ESVs have not been systematically investigated, despite the intense human economic activity so far. Therefore, the purpose of this paper is (1) to propose GEE-based land-use changes and an ESV dynamic analysis framework, (2) to analyze the land-use change characteristics using this framework, and (3) to investigate ESV dynamics in the SMA. The result would provide helpful information to future ecosystem management policymaking in the SMA.

2. Materials and Methods

2.1. Study Area

The SMA is located in central-north Liaoning Province, in the northeast of China (122°24′ E–125°47′ E, 40°00′ N–43°02′ N), with an area of 37,280 km^2 (Figure 1). The SMA was set as one of the National Comprehensive Reform Pilot Zones by China's State Council in 2010. It initially consisted of eight prefecture-level cities, and was adjusted to five in 2017: Shenyang city (the capital of Liaoning Province), Benxi city, Anshan city, Fushun city, and Liaoyang city. To the east and south of SMA are the Qianshan Mountains (a branch of the Changbai Mountains), while to the west and north is the Liaohe Plain (a part of the North China Plain). The SMA has a monsoon-influenced hot-summer humid continental climate (Dwb), with four distinctive seasons. In 2019, the average annual temperature was 9.8 °C. The average monthly temperature extended from −7.2 °C in January to 26.1 °C in July. The yearly precipitation was 786.5 mm [42,43]. As an important agricultural area in Liaoning Province, the total grain output of the SMA in 2019 was 6.433 million tons, accounting for 39% of the grain output of Liaoning Province. The grain crops are mainly corn and rice, accounting for more than 95% of the total grain output. The SMA is also an important political and economic center in northeast China. In recent decades, the SMA has experienced rapid industrialization and urbanization. The population increased from 15.9 million in 2000 to 16.2 million in 2019, and the gross domestic product (GDP) rose from 2277.53 hundred million Chinese Yuan (hmCYN) to 10,674.8 hmCYN in 2019 [42,43].

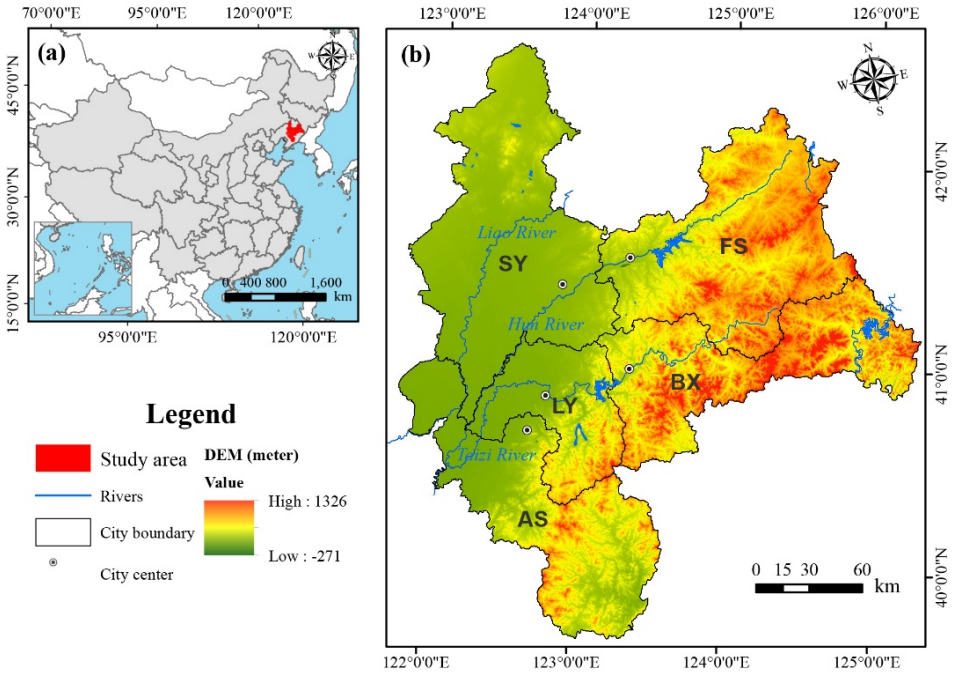

Figure 1. (**a**) Location of the Shenyang Metropolitan Area in China and (**b**) its administrative division and topographical map. SY: Shenyang city; FS: Fushun city; LY: Liaoyang city; BX: Benxi city; AS: Anshan city.

2.2. Overall Workflow

The study consists of two primary steps (Figure 2): land-use changes analysis based on the GEE platform, and ESV changes evaluation based on a spatiotemporal adjusted value transfer method. We discuss both parts briefly, in Sections 2.3 and 2.4, respectively.

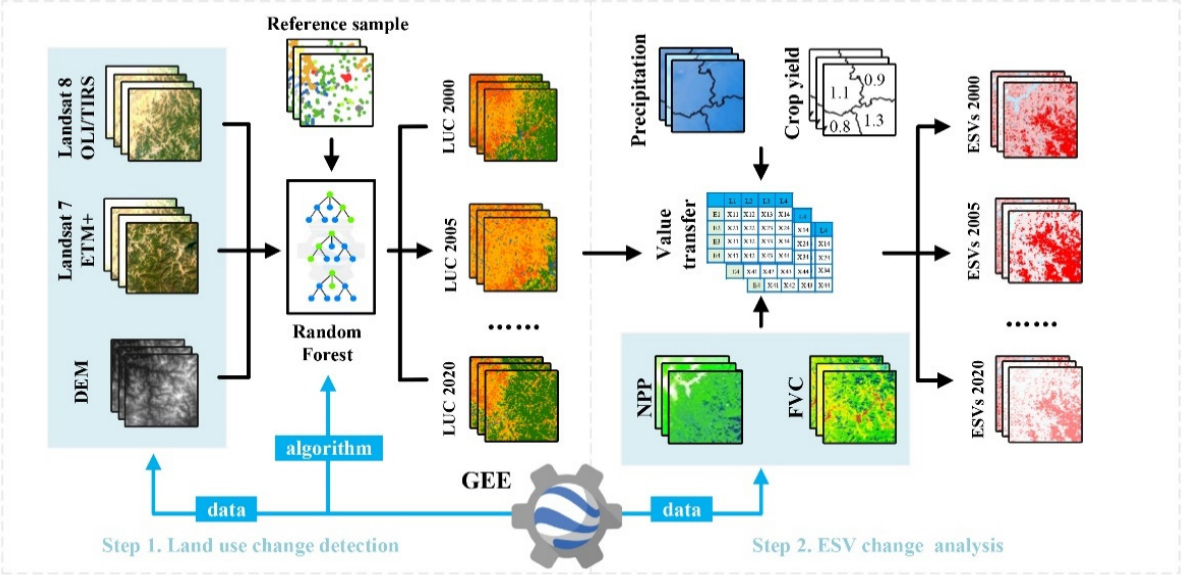

Figure 2. The overall workflow of the study. GEE: Google Earth Engine; DEM: digital elevation model; LUC: land-use change; NPP: net primary productivity; FVC: fractional vegetation cover; ESV: ecosystem service value.

2.3. The Process of Land-Use Change Analysis in GEE

2.3.1. Data Acquisition and Processing

We classified the land use of the SMA on the GEE platform for the years 2000, 2005, 2010, 2015, and 2020. We depicted the general procedures in Figure 3. With a nominal resolution of 30 meters and a temporal granularity of 16 days, Landsat is one of the most commonly used remote sensing data for land use classification [21,23,44]. In contrast, GEE has free access to decades of global coverage of Landsat dataset, including Landsat 4–8 surface reflectance (1984–now), Landsat 5 TM (1984–2012), Landsat 7 ETM+ (1999–now), and Landsat 8 OLI/TIRS (2013–now) [20]. This study employed Landsat 7 Surface Reflectance Tier 1 from the Landsat 7 database, and Landsat 8 Surface Tier 1 from the Landsat 8 databases. We selected 11 scenes, based on the study area boundary. Figure 4a shows the spatial ground coverage of the selected scenes, including their path and row number. We excluded images with cloud cover greater than 20%. The time interval of the image was from March 1st to October 31st, when the SMA is snow-free. As the image quality usually suffers from high cloud cover, resulting in empty pixels or scenes, we adapted the dense stacking approach [29,30,45]. We finally screened out 633 scenes of Landsat images to composite land use data for 2000 (104 scenes), 2005 (139 scenes), 2010 (128 scenes), 2015 (162 scenes), and 2020 (100 scenes) (more details listed in Table S1). To increase the classification accuracy, we also included the digital elevation model (DEM), slope, normalized difference vegetation index (NDVI) [46], and normalized difference water index (NDWI) [47] into the classification framework. The DEM data were from NASA SRTM Digital Elevation 30m databases in GEE. The slope data were derived from DEM, using the slope function provided by GEE. NDVI and NDWI were obtained through band calculation in GEE.

2.3.2. Image Classification and Accuracy Assessments

We identified six land-use types: water body, forest land, built-up area, cropland, grassland, and unused land. The land-use classification scheme was based on China's Multi-Period Land Use Land Cover Remote Sensing Monitoring Data Set (CNLUCC) [48]. The description for each land-use type is listed in Table S2. Next, we prepared the reference points using visual interpretation of the high-resolution history images of Google Earth in different years. In total, we obtained over 3600 reference points, and their spatial distribution is shown in Figure 4b. Then, we employed the random forest algorithm as

the land-use classification classifier. The random forest classifier is well known for its efficiencies and accuracy, even with more substantial data noise [49,50]. We trained the random forest classifier using 70% of the reference data, and 30% for model validation. Finally, we employed the producer's accuracy, user's accuracy, and kappa coefficient [51] to examine the accuracy of the classification results.

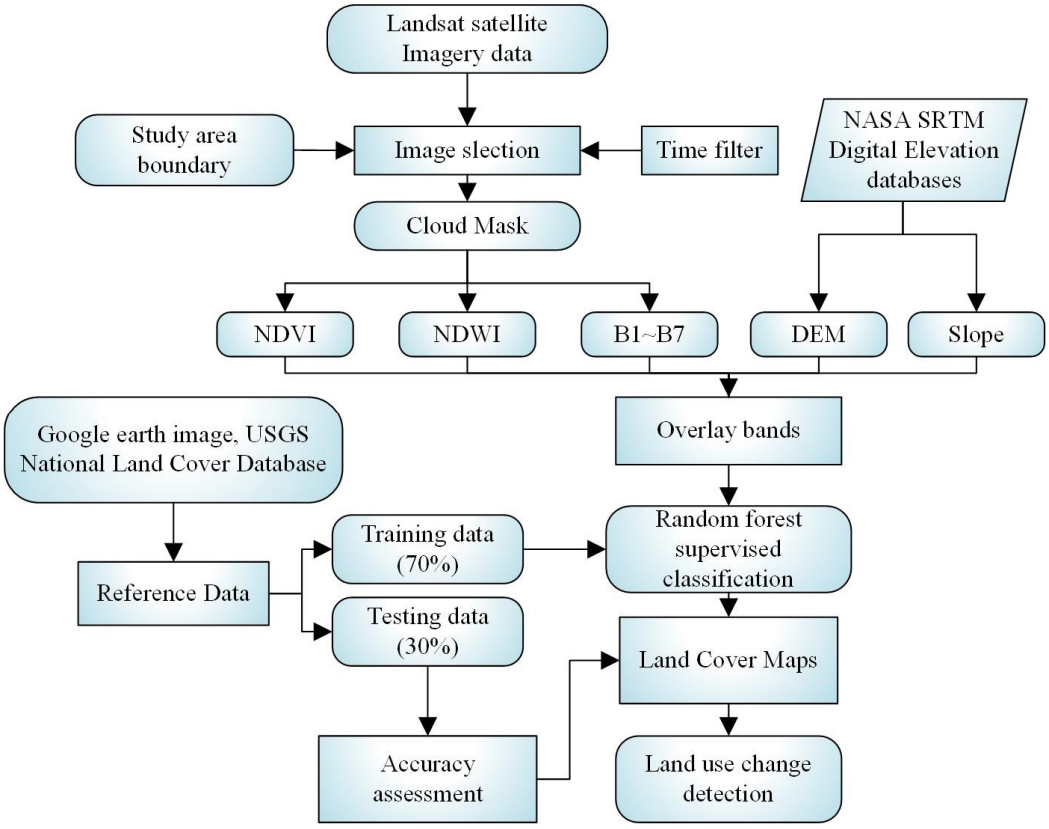

Figure 3. Flow chart of land-use classification using Google Earth Engine.

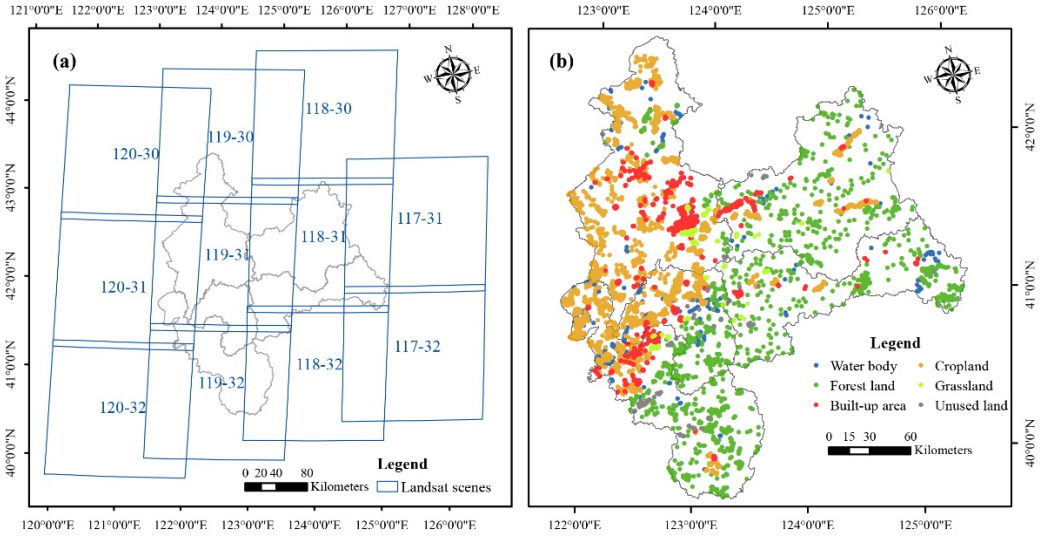

Figure 4. (**a**) Landsat scene coverage and (**b**) spatial distribution of the reference points of the study area.

2.4. Assessment of the Ecosystem Service Values Changes

2.4.1. The Equivalent Table and Standard Value Factors

We quantified the ESVs based on the equivalent table method [32,35,36]. Overall, eleven ecosystem service functions were studied: food supply, raw material supply, water supply, air regulation, climate regulation, purifying the environment, hydrology adjustment, soil formation, nutrient cycling, biological control, and culture and amenity. The equivalent factors of the six land-use types for the eleven ecosystem service functions are listed in Table S3. The method took the economic value of food production per unit area of the cropland as the standard equivalent value factor using the following equation:

$$E_a = \frac{1}{7} \times \frac{\sum_{i=1}^{n} m_i \times p_i \times q_i}{\sum_{i=1}^{n} m_i} \quad (1)$$

where E_a is the standard equivalent value factor (Chinese Yuan·ha^{-1} (CNY·ha^{-1})); i represents the crop type; and m, p, and q represent the sown area (ha), the average market price (CNY·Kg^{-1}), and the crop yield per unit (kg·ha^{-1}), respectively. We included three types of grain (corn, rice, and bean) for the calculation, as their output accounted for more than 97% of the total grain output in the SMA. The prices and production of agricultural product data were from China's Agricultural Product Cost-benefit Data, the China Statistical Yearbook, Liaoning Statistical Yearbook, and Grain Statistics Announcement by the National Bureau of Statistics of China. We used the average price to eliminate the impact of price inflation. Finally, the economic values of one weight factor for 2000, 2005, 2010, 2015, and 2020 were 1247.8 CNY·ha^{-1}, 1677.6 CNY·ha^{-1}, 1506.6 CNY·ha^{-1}, 1605.6 CNY·ha^{-1}, and 1722.8 CNY·ha^{-1}, respectively.

2.4.2. Spatiotemporal Correction Factors

We adopted NPP, FVC, crop yield, and precipitation to adjust the equivalent coefficients based on previous work [32,40,41]. We have listed the equations, the corresponding relationship between the correction coefficients and ecosystem service functions, and the data sources in Table 1. The spatial distributions of correction factors for the years 2000, 2005, 2010, 2015, and 2020 are shown in Figure 5.

Table 1. Equations and the corresponding and data sources of the correction factors.

Correction Factors	Equations		Ecosystem Service Functions	Data Sources
Net primary productivity (NPP)	$EF_{NPP} = \frac{NPP_i}{NPP_C}$	EF_{NPP} is the correction factor of NPP; NPP_i and NPP_C represent the NPP value at the study location and average NPP value of China.	Raw material supply, air regulation, climate regulation, purifying environment, nutrient cycling, biological control, and culture and amenity	NPP was from the MOD17A3HGF V6 database in GEE.
Fractional vegetation cover (FVC)	$EF_{FVC} = \frac{FVC_i}{FVC_C}$ $FVC = \frac{NDVI - NDVI_{\min}}{NDVI_{\max} - NDVI_{\min}}$	EF_{FVC} is the correction factor of fractional vegetation cover; FVC is the fractional vegetation cover; FVC_i and FVC_C represent the fractional vegetation cover at the study location and the annual average value of China; and $NDVI$ represents the Normalized Difference Vegetation Index.	Soil formation	$NDVI$ was from the MOD13A2 V6 database in GEE.

Table 1. *Cont.*

Correction Factors	Equations		Ecosystem Service Functions	Data Sources
Crop yield	$EF_Y = \frac{Y_i}{Y_C}$	EF_Y is the correction factor of crop yield; Yi and Yc represent the crop yield at the study location and the annual average value of China.	Food supply	The crop yield data were from the China Statistical Yearbook, Liaoning Statistical Yearbook, and Grain Statistics Announcement by the National Bureau of Statistics of China.
Precipitation	$EF_P = \frac{P_i}{P_C}$	EF_P is the correction factor of precipitation; P_i and P_c represent the annual precipitation at the study location and the annual precipitation average of China.	Water supply and water regulation	The precipitation data were from National Earth System Science Data Center, China's National Science and Technology Infrastructure.

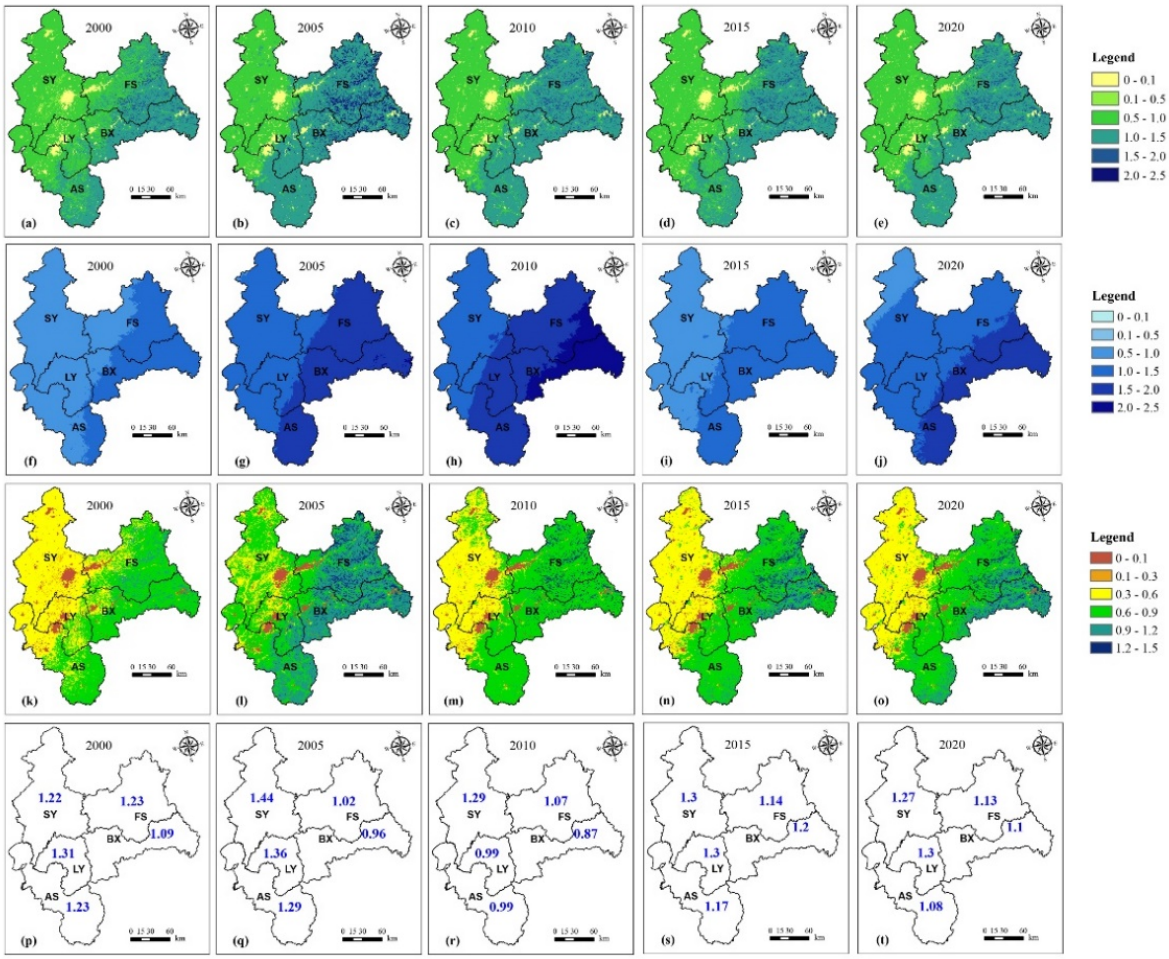

Figure 5. Spatiotemporal correction factor maps of (**a**–**e**) net primary productivity (2000, 2005, 2010, 2015, and 2020); (**f**–**j**) fractional vegetation cover (2000, 2005, 2010, 2015, and 2020); (**k**–**o**) precipitation (2000, 2005, 2010, 2015, and 2020); and (**p**–**t**) crop yield (2000, 2005, 2010, 2015, and 2020).

2.4.3. ESV Calculation and Change Analysis

Finally, the total ESVs were calculated using the following equations:

$$ESV_k = \sum_f A_k \times EF_f \times VC_{kf} \quad (2)$$

$$ESV_f = \sum_k A_k \times EF_f \times VC_{kf} \quad (3)$$

$$ESV = \sum_{k}\sum_{f} A_k \times EF_f \times VC_{kf} \quad (4)$$

where ESV_k represents the ecosystem service value of the land-use type k (CNY), ESV_f is the ecosystem service value of ecosystem service function f (CNY), and ESV is the total of the ecosystem service values (CNY). EF is the correction factor of ecosystem service function f. A_k is the land-use type k area (ha), and VC_{kf} is the unit value for ecosystem service function f of land use type k [12,41,52].

After that, the change rate of ESV was measured as follows:

$$\Delta ESV_{T_1-T_2}(\%) = \frac{ESV_{T_2} - ESV_{T_1}}{ESV_{T_1}} \times 100\% \quad (5)$$

where $\Delta ESV_{T_1-T_2}$ is the change rate of ESV from the years T_1 to T_2 (%), and ESV_{T_1} and ESV_{T_2} are the ecosystem service values in the years T_1 and T_2 (Yuan) [41].

2.4.4. Coefficient Sensitivity Assessment

Finally, we used the coefficient of sensitivity (CS) to examine the uncertainties using the following equation [53]:

$$CS = \frac{\left(ESV_j - ESV_i\right)/ESV_i}{\left(VC_{jk} - VC_{ik}\right)/VC_{ik}} \quad (6)$$

where ESV_j and ESV_i are the initial and adjusted ecosystem service values (CNY). k represents the land-use type. If CS is greater than one, the estimated ESV is considered elastic. However, if CS is less than one, the estimated ESV could be treated as inelastic, indicating the robustness and reasonability of the ESV calculation [33,53–55].

3. Results

3.1. Land-Use Changes in the Shenyang Metropolitan Area

We depicted the land-use classification results for the years 2000, 2005, 2010, 2015, and 2020 in Figure 6, and listed the statistical summary in Table 2. Forest land, mainly distributed in the east and south, was the predominant land-use type in the SMA in all five periods, accounting for 45.39% (21,120 km^2), 45.18% (21,019 km^2), 44.92% (20,900 km^2), 44.18% (20,558 km^2), and 44.30% (20,604 km^2) for the years 2000, 2005, 2010, 2015, and 2020, respectively. Cropland was the second largest land-use type, accounting for 45.35% (21,101 km^2), 44.33% (20,625 km^2), 43.55% (20,262 km^2), 43.32% (20,154 km^2), and 42.56% (19,796 km^2), respectively, and was mainly concentrated in the north and west. The built-up area was primarily located in the central area, and occupied 2727 km^2 (5.86%), 3038 km^2 (6.53%), 3533 km^2 (7.59%), 4081 km^2 (8.77%), and 4601 km^2 (9.89%) in 2000, 2005, 2010, 2015, and 2020, respectively, making it the third largest land-use type. Water, grassland, and unused land did not illustrate apparent spatial distribution characteristics, and all covered a small proportion, with a five-period average proportion of 1.76% (817 km^2), 1.58% (734 km^2), and 0.32% (149 km^2), respectively.

Figure 7 illustrates the area and proportion change of land use from 2000 to 2020. The built-up area increased rapidly, and the change rates were 11.4%, 16.31%, 15.51%, and 12.74% for 2000–2005, 2005–2010, 2010–2015, and 2015–2020, respectively, resulting in the largest area gain (1874.43 km^2) (Table S4). In contrast, a significant decline trend was found in cropland (−2.25%, −1.76%, −0.53%, and −1.78% for 2000–2005, 2005–2010, 2010–2015, and 2015–2020, respectively), causing the largest overall area reduction (−1305.09 km^2). The forest land decreased in 2000–2005 (−0.48%), 2005–2010 (−0.57), and 2010–2015 (−1.64%), and increased slightly in 2015–2020 (0.23%), resulting in an overall area loss of −516.32 km^2. The grassland experienced a substantial expansion in 2000–2005 (20.6%), and kept decreasing in 2005–2020, resulting in an overall area loss of 201.66 km^2 (−27.47%). The water body grew significantly in 2000–2005 and 2010–2015, descended in 2005–2010 and 2015–2020,

and finally increased by 85.85 km^2 (11.74%). The unused land increased from 2000 to 2015, and substantially declined in 2015–2020, with an overall increase of 45.21 km^2 from 2000 to 2020.

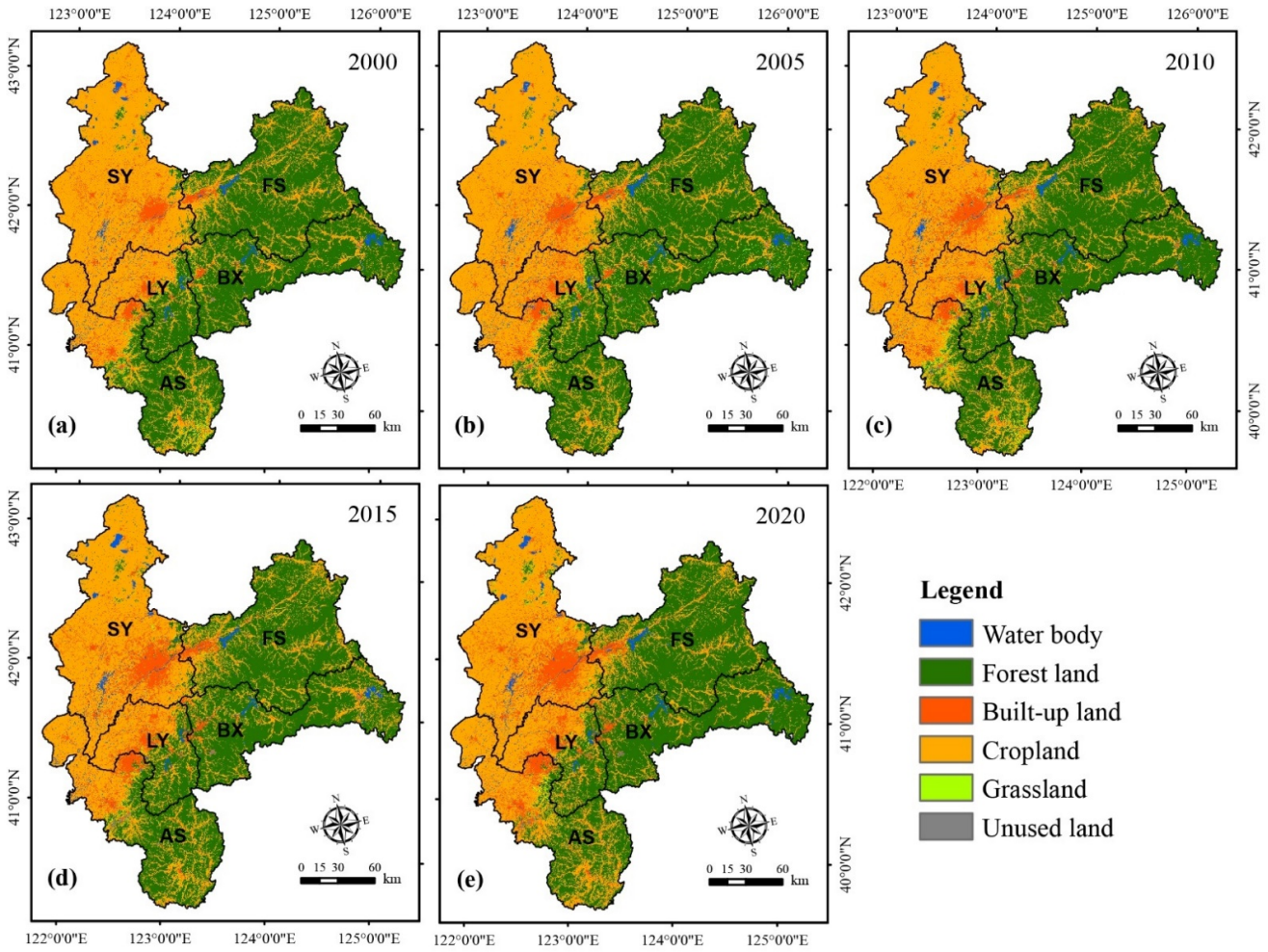

Figure 6. Spatial distribution of land-use categories for the years (**a**) 2000, (**b**) 2005, (**c**) 2010, (**d**) 2015, and (**e**) 2020.

Table 2. Statistical summary of land use classifications (km^2).

	2000		2005		2010		2015		2020		Average	
Land-Use Type	**Area**	**%**	**Area**	**%**	**Area**	**%**	**Area**	**%**	**Area**	**%**	**Area**	**%**
Water	731	1.57	842	1.81	822	1.77	874	1.88	817	1.76	817	1.76
Forest	21,120	45.39	21,019	45.18	20,900	44.92	20,558	44.18	20,604	44.30	20,840	44.79
Built-up area	2727	5.86	3038	6.53	3533	7.59	4081	8.77	4601	9.89	3596	7.73
Cropland	21,101	45.35	20,625	44.33	20,262	43.55	20,154	43.32	19,796	42.56	20,388	43.82
Grassland	734	1.58	885	1.90	845	1.82	672	1.44	532	1.14	734	1.58
Unused land	114	0.25	118	0.25	166	0.36	188	0.40	160	0.34	149	0.32

The overall accuracies for classification maps for the year 2000, 2005, 2010, 2015, and 2020 were 97.8%, 94.7%, 96.1%, 97.1%, and 96.2%, respectively, and the overall kappa coefficients for each year were 0.968, 0.966, 0.941, 0.956, and 0.939, respectively (Table 3). In addition to the low accuracy of the grassland, all of the producer's accuracy and the consumer's accuracy are higher than 90%.

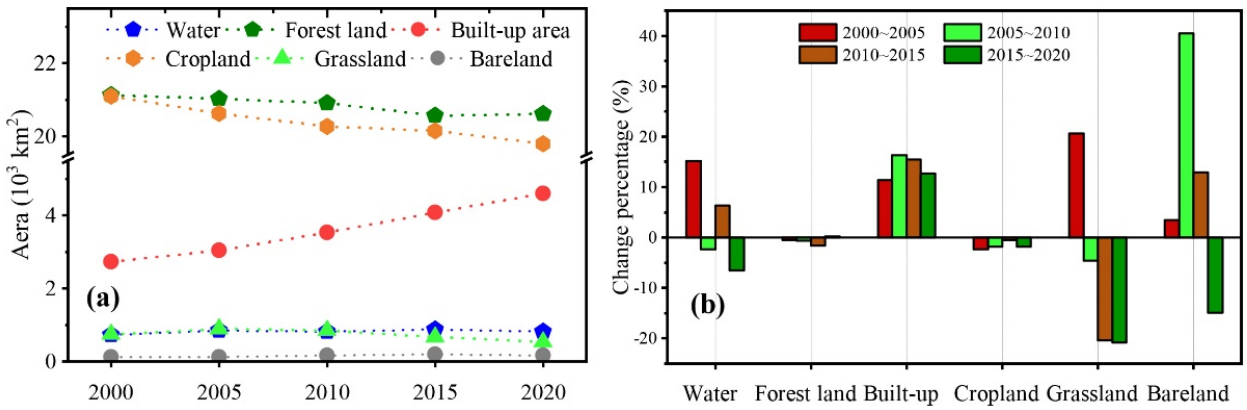

Figure 7. Land-use changes (**a**) by area and (**b**) by proportion.

Table 3. The results of the classification accuracy assessment.

	2000		2005		2010		2015		2020	
Land-Use Type	**PA**	**CA**	**PA**	**CA**	**PA**	**CA**	**PA**	**CA**	**PA**	**CA**
Water body	0.957	0.987	0.987	0.989	0.918	0.949	0.947	0.981	0.964	0.987
Forest land	0.981	0.98	0.976	0.967	0.982	0.962	0.996	0.993	0.943	0.953
Built-up area	0.97	0.992	0.941	0.962	0.941	0.965	0.951	0.97	0.953	0.973
Cropland	0.993	0.97	0.982	0.963	0.989	0.962	0.989	0.969	0.98	0.949
Grassland	0.733	0.916	0.613	0.95	0.672	0.886	0.777	0.907	0.696	0.941
Unused land	0.971	0.943	0.98	0.981	0.924	0.973	0.969	0.984	0.963	0.987
Overall accuracy	0.978		0.947		0.961		0.971		0.962	
Kappa coefficient	0.968		0.966		0.941		0.956		0.939	

PA: producer's accuracy; CA: consumer's accuracy.

3.2. Spatiotemporal Changes in Ecosystem Service Values

Figure 8 depicts the spatial distribution of ESVs of the SMA in the years 2000, 2005, 2010, 2015, and 2020. The ESVs were high in the eastern and northern regions, and low in the west and south. The total ESVs in 2000, 2005, 2010, 2015, and 2020 are 814.04 hmCNY, 1546.82 hmCNY, 1283.78 hmCNY, 1145.76 hmCNY, and 1329.81 hmCNY, respectively (Figure 9a and Table S5). The ESVs of forest land comprised the largest portion (Figure 9b), with the percentage ranging from 72.65% to 77.18%, followed by water, ranging from 11.61% to 15.64%, and cropland, ranging from 8.45% to 9.93%. The ESVs for ecosystem service functions are shown in Figure 9c and Table S6. ESVs for hydrology adjustment (ranging from 22.60% to 28.86%) and ESV climate regulation (ranging from 22.12% to 24.89%) are the two most significant contributors to the overall ESVs, followed by biological control (ranging from 8.27% to 9.73%), gas regulation (ranging from 8.51% to 9.99%), soil formation (ranging from 7.52% to 8.94%), and purifying the environment (6.51% to 7.63%). Ecosystem service functions with the least ESVs were raw material supply, water supply, and nutrient cycling, with a five-period average value of 39.26 hmCNY (3.12%), 31.60 hmCNY (2.54%), and 12.07 hmCNY (0.99%), respectively.

We illustrate the spatial and temporal ESV changes in 2000–2005, 2005–2010, 2010–2015, 2015–2020, and 2000–2020 in Figures 10 and 11, and their statistical summary in Tables S7 and S8. The most dynamic change areas of ESVs were located mainly in the eastern and northern regions. The overall ESVs had a substantial increase (732.78 hmCNY, 90.02%) from 2000 to 2005, then declined by −17.01% (−263.04 hmCNY) in the period between 2005 and 2010, and by −10.75% (−138.02 hmCNY) in 2010–2015, and finally increased significantly in 2015–2020 (184.05 hmCNY). The ESV change in forest land comprised most of the variations of the total ESV in all four periods. ESV changes in water were the second contributor to the ESV change in 2000–2005, 2010–2015, and 2015–2020. In contrast, from 2005 to 2010, the decrease in ESVs of cropland (−27.22 hmCNY) contributed the second most to the loss in total ESVs. From the

perspective of overall ESV changes from 2000 to 2020, forest land comprised the most ESV changes (365.57 hmCNY), followed by water body (113.41 hmCNY), cropland (36.11 hmCNY), and grassland (0.66 hmCNY). However, from the perspective of the degree of changes, the water body ranked first (119.96%), followed by forest land (58.19%) and cropland (44.65%) (Table S4). Hydrology adjustment and climate regulation were the primary ecosystem service functions with the most significant ESV changes, with overall changes of 199.87 hmCNY and 101.68 hmCNY, respectively, followed by soil formation (43.95 hmCNY) and gas regulation (38.55 hmCNY). While from the perspective of the degree of changes, ecosystem functions with the most changes by percentage were hydrology adjustment (108.85%), followed by water supply (107.33%), and soil formation (64.83%).

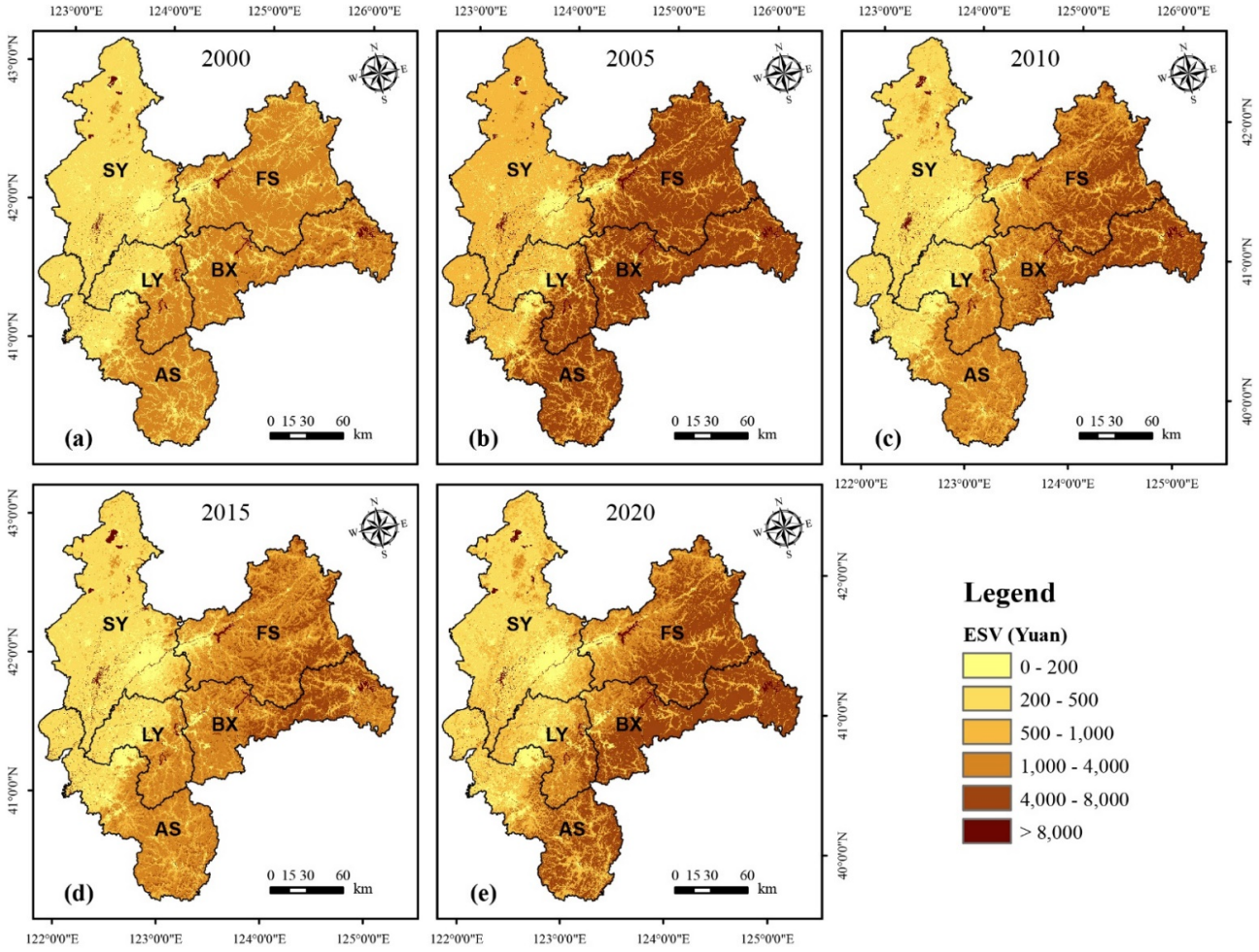

Figure 8. Spatial distribution of ESVs in (**a**) 2000, (**b**) 2005, (**c**) 2010, (**d**) 2015, and (**e**) 2020.

3.3. Ecosystem Service Values in the Prefecture-Level Cities

Fushun had the highest ESVs among the five prefecture-level cities of the SMA, with a five-period average value of 420.08 hmCNY, followed by Benxi (362.65 hmCNY), Anshan (212.32 hmCNY), Shenyang (124.02 hmCNY), and Liaoyang (104.94 hmCNY) (Figure 12). The ESV dynamics of the five cities were the same as that of the entire SMA region, which increased in 2000–2005, descended in 2005–2015, and ascended finally in 2015–2020. The ESVs of forest land constituted the most significant portion of ESVs in Anshan (ranging from 74.21%–77.65%), Fushun (89.47%–89.10%), Benxi (80.97%–85.95%), and Liaoyang (58.77%–65.89%), while for Shenyang, the highest ESVs were associated with water bodies (37.8%–52.09%) and cropland (38%–51.22%) (Table S9). Hydrology adjustment and climate regulation were the primary ecosystem service functions for Anshan (jointly accounting for 46.5%–52.5%), Fushun (47.7%–52.9%), Benxi (50.9%–57.8%), and Liaoyang

(51.3%–59.5%) (Table S10). In contrast, for Shenyang, hydrology adjustment and food supply together comprised 58.2%–64.6% of the total ESV (more information can be found in Tables S9 and S10).

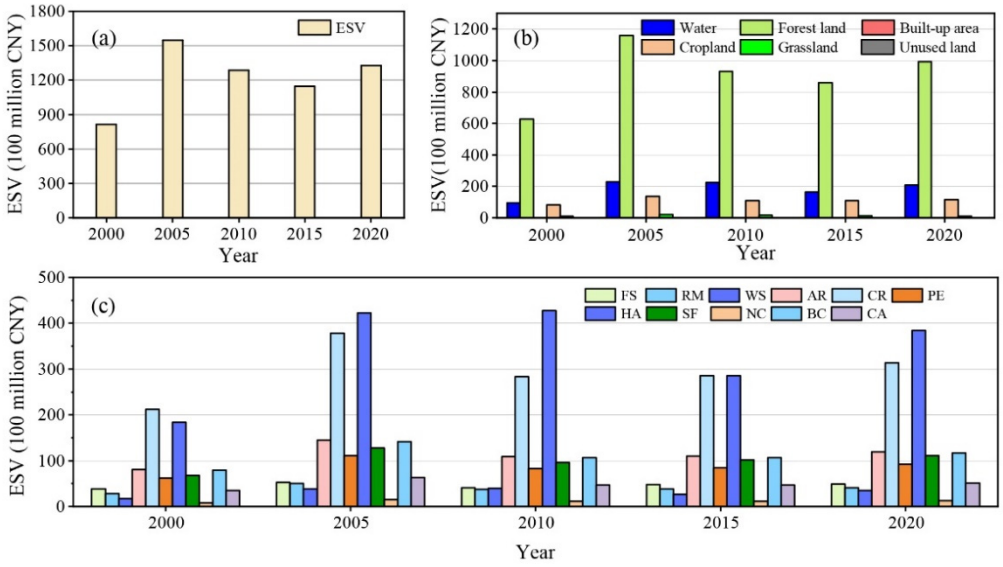

Figure 9. (**a**) Total ecosystem service values by years, (**b**) ecosystem service values by land-use type, and (**c**) ecosystem service values of different ecosystem service functions. FS: Food supply, RM: raw material supply, WS: water supply, AR: air regulation, CR: climate regulation, PE: purifying the environment, HA: hydrology adjustment, SF: soil formation, NC: nutrient cycling, BC: biological control, CA: culture and amenity.

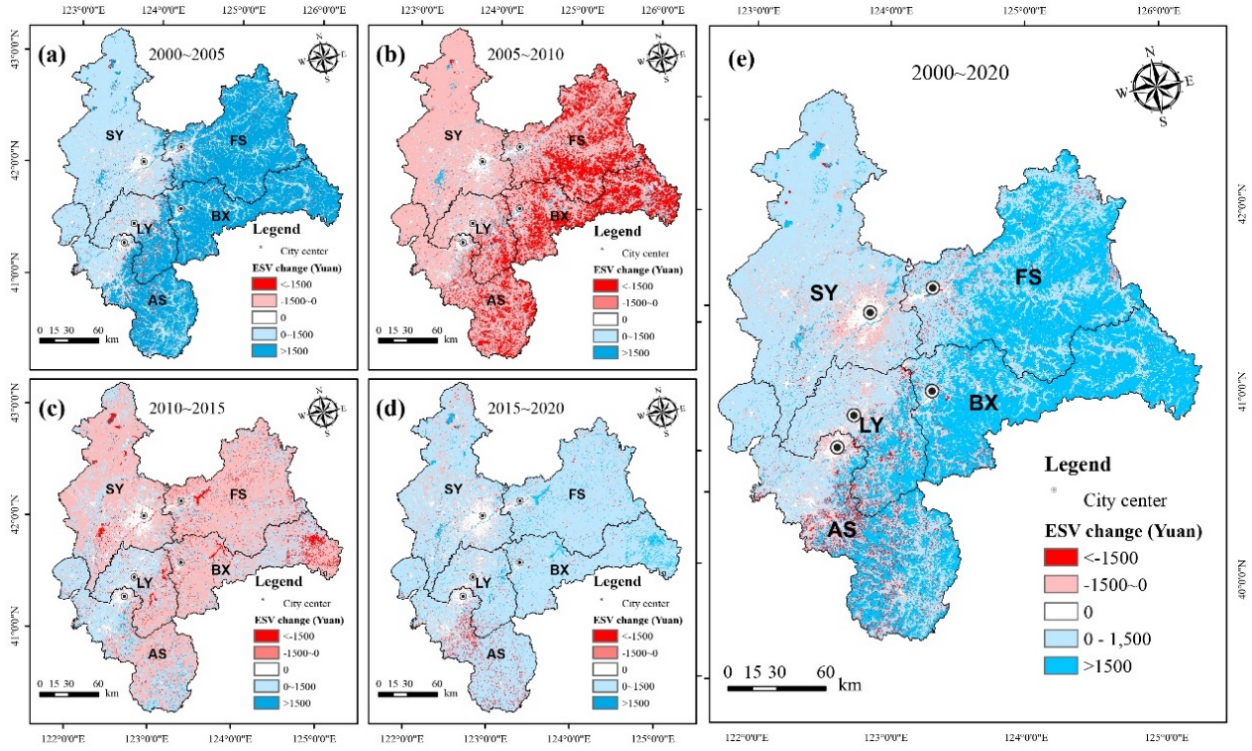

Figure 10. The spatial change of ecosystem service values in the periods (**a**) 2000–2005, (**b**) 2005–2010, (**c**) 2010–2015, (**d**) 2015–2020, and (**e**) 2000–2020.

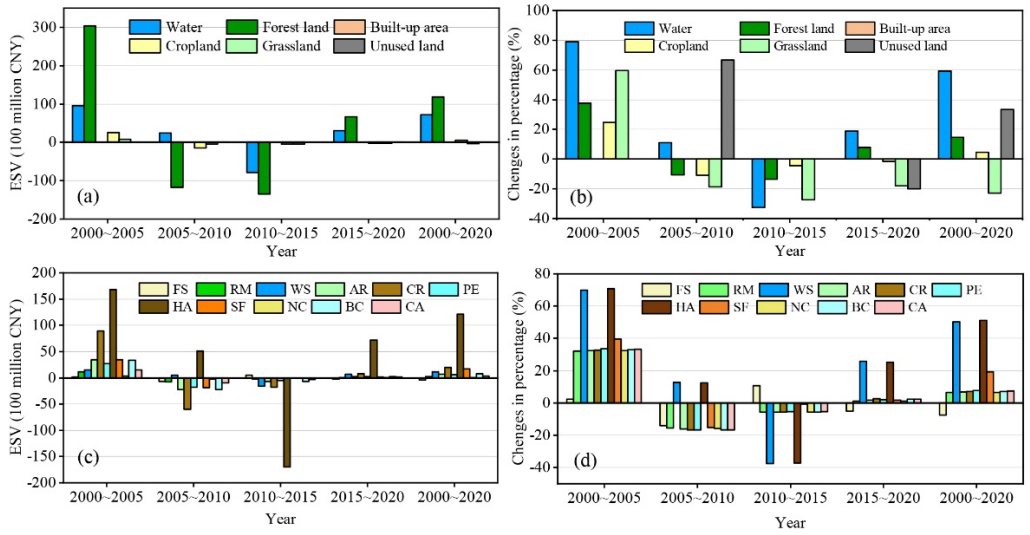

Figure 11. (**a**) ESV changes by land-use type, (**b**) ESV percentage changes by land-use type, (**c**) ESV changes by ecosystem service functions, and (**d**) ESV percentage changes by ecosystem service functions. FS: Food supply, RM: raw material supply, WS: water supply, AR: air regulation, CR: climate regulation, PE: purifying the environment, HA: hydrology adjustment, SF: soil formation, NC: nutrient cycling, BC: biological control, CA: culture and amenity.

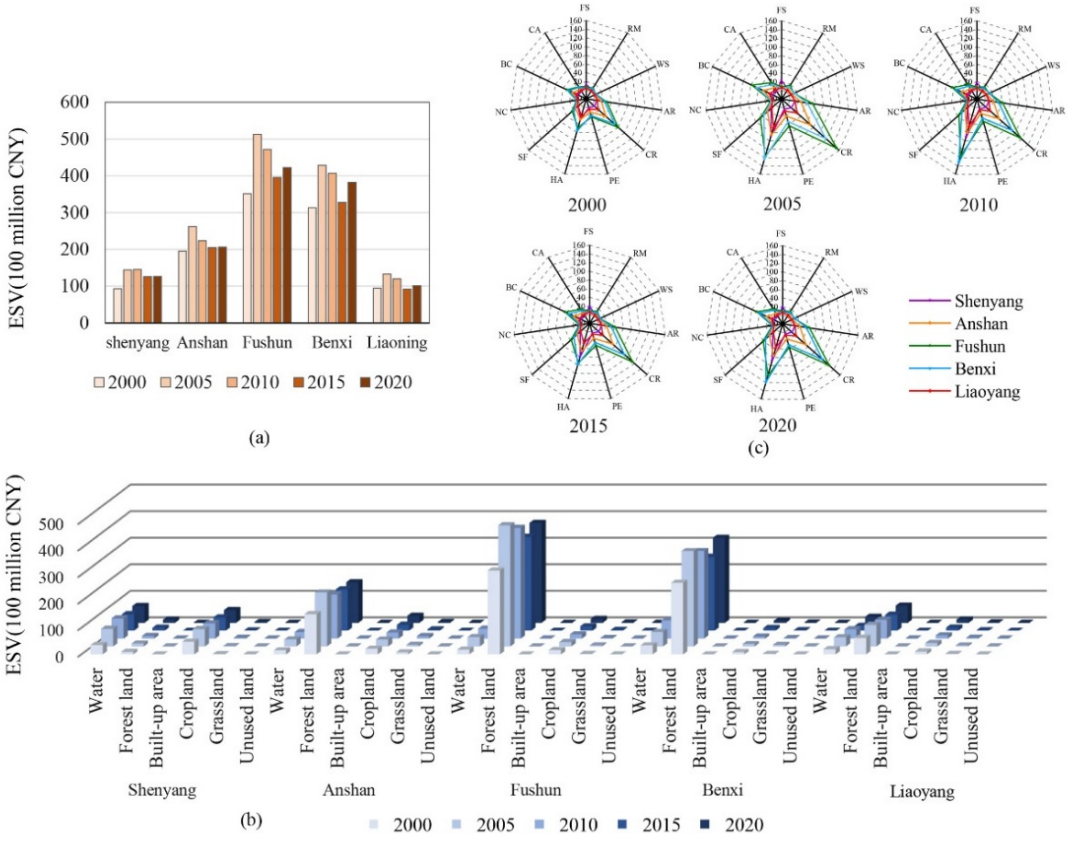

Figure 12. (**a**) Ecosystem service values of the prefecture-level cities by year, (**b**) ecosystem service values of land-use types of the prefecture-level cities, and (**c**) ecosystem service values of ecosystem service functions of the prefecture-level cities. FS: Food supply, RM: raw material supply, WS: water supply, AR: air regulation, CR: climate regulation, PE: purifying the environment, HA: hydrology adjustment, SF: soil formation, NC: nutrient cycling, BC: biological control, CA: culture and amenity.

3.4. Sensitivity Assessment

The sensitivity assessment indicates that the CS of six land-use types was less than one in all cases (Table 4). In all five periods, the CS of forest land ranked first, with an average value of 0.749, followed by water body (0.148), cropland (0.091), grassland (0.012), unused land (0.000), and built-up areas (0.000).

Table 4. The coefficient of the sensitivity value of different land uses for 2000, 2005, 2010, 2015, and 2020.

Year	Coefficient of Sensitivity					
	Water	**Forest Land**	**Built-Up Area**	**Cropland**	**Grassland**	**Unused Land**
2000	0.116	0.772	0.000	0.099	0.013	0.000
2005	0.147	0.751	0.000	0.088	0.014	0.000
2010	0.176	0.727	0.000	0.085	0.013	0.000
2015	0.142	0.750	0.000	0.097	0.011	0.000
2020	0.156	0.747	0.000	0.088	0.008	0.000
Average	0.148	0.749	0.000	0.091	0.012	0.000

Table 5 represents the CS of different ecosystem service functions. The CS of forest land was highest for most of the ecosystem service functions, including food supply, raw material supply, water supply, air regulation, climate regulation, purifying the environment, hydrology adjustment, soil formation, nutrient cycling, biological control, and culture and amenity. The CS of cropland was found to be highest for the food supply function, while for hydrology adjustment in 2015, the water body was associated with the highest CS.

Table 5. The coefficient of sensitivity values of ecosystem service function for the years 2000, 2005, 2010, 2015, and 2020.

Ecosystem Service Function	Years	Coefficient of Sensitivity					
		Water Body	**Forest Land**	**Built-Up Area**	**Cropland**	**Grassland**	**Unused Land**
Food supply	2000	0.023	0.254	0.000	0.716	0.007	0.000
	2005	0.027	0.225	0.000	0.740	0.008	0.000
	2010	0.026	0.237	0.000	0.730	0.008	0.000
	2015	0.029	0.251	0.000	0.714	0.006	0.000
	2020	0.027	0.253	0.000	0.714	0.005	0.000
Raw material	2000	0.003	0.721	0.000	0.265	0.011	0.000
	2005	0.004	0.723	0.000	0.262	0.012	0.000
	2010	0.004	0.715	0.000	0.270	0.011	0.000
	2015	0.004	0.715	0.000	0.271	0.009	0.000
	2020	0.004	0.729	0.000	0.260	0.007	0.000
Water supply	2000	0.385	0.581	0.000	0.025	0.009	0.000
	2005	0.410	0.556	0.000	0.023	0.011	0.000
	2010	0.410	0.557	0.000	0.022	0.010	0.000
	2015	0.432	0.537	0.000	0.023	0.008	0.000
	2020	0.414	0.557	0.000	0.023	0.006	0.000
Gas regulation	2000	0.004	0.829	0.000	0.154	0.013	0.000
	2005	0.004	0.829	0.000	0.152	0.015	0.000
	2010	0.004	0.825	0.000	0.158	0.013	0.000
	2015	0.005	0.825	0.000	0.158	0.012	0.000
	2020	0.005	0.836	0.000	0.151	0.009	0.000

Table 5. *Cont.*

Ecosystem Service Function	Years	Coefficient of Sensitivity					
		Water Body	Forest Land	Built-Up Area	Cropland	Grassland	Unused Land
Climate regulation	2000	0.004	0.950	0.000	0.032	0.014	0.000
	2005	0.005	0.949	0.000	0.031	0.015	0.000
	2010	0.005	0.949	0.000	0.033	0.014	0.000
	2015	0.006	0.950	0.000	0.033	0.012	0.000
	2020	0.005	0.955	0.000	0.031	0.009	0.000
Purifying environment	2000	0.036	0.919	0.000	0.030	0.015	0.000
	2005	0.041	0.912	0.000	0.029	0.017	0.000
	2010	0.041	0.913	0.000	0.031	0.015	0.000
	2015	0.046	0.910	0.000	0.031	0.013	0.000
	2020	0.042	0.918	0.000	0.029	0.010	0.000
Hydrology adjustment	2000	0.443	0.515	0.000	0.032	0.011	0.000
	2005	0.469	0.490	0.000	0.028	0.013	0.000
	2010	0.470	0.491	0.000	0.028	0.011	0.000
	2015	0.492	0.470	0.000	0.029	0.009	0.000
	2020	0.474	0.490	0.000	0.029	0.007	0.000
Soil formation	2000	0.004	0.795	0.000	0.189	0.013	0.000
	2005	0.004	0.797	0.000	0.184	0.014	0.000
	2010	0.004	0.792	0.000	0.191	0.013	0.000
	2015	0.005	0.792	0.000	0.192	0.011	0.000
	2020	0.004	0.804	0.000	0.183	0.008	0.000
Nutrient cycling	2000	0.003	0.727	0.000	0.259	0.011	0.000
	2005	0.004	0.728	0.000	0.255	0.013	0.000
	2010	0.004	0.721	0.000	0.264	0.011	0.000
	2015	0.004	0.721	0.000	0.265	0.010	0.000
	2020	0.004	0.735	0.000	0.254	0.008	0.000
Biological control	2000	0.013	0.941	0.000	0.031	0.015	0.000
	2005	0.015	0.938	0.000	0.030	0.017	0.000
	2010	0.015	0.939	0.000	0.032	0.015	0.000
	2015	0.017	0.939	0.000	0.032	0.013	0.000
	2020	0.015	0.945	0.000	0.030	0.010	0.000
Culture and amenity	2000	0.022	0.931	0.000	0.032	0.015	0.000
	2005	0.025	0.927	0.000	0.031	0.017	0.000
	2010	0.024	0.928	0.000	0.033	0.015	0.000
	2015	0.028	0.926	0.000	0.033	0.013	0.000
	2020	0.026	0.933	0.000	0.031	0.010	0.000

4. Discussion

4.1. Land Use Changes and ESV Dynamics

Accurate land-use change data are a prerequisite for ecosystem service assessments. This study used the Landsat dense stacking methodology and the random forest supervised classification algorithm within the GEE platform to analyze the land-use changes in a regional-scale case study in 2000, 2005, 2010, 2015, and 2020. The overall accuracy ranged from 94.7% to 97.8%, and the kappa coefficient ranged from 0.939 to 0.968. The results indicate that the method accurately classified the land use, and could provide a valid reference to analyze the characteristics of the land-use changes.

According to the classification result, the dominant land-use types in the SMA region were forest land and cropland, which jointly occupied 75%–89% of the total area. The forest land is mainly distributed in the eastern and southern mountain regions, while the cropland concentrates primarily on the northern and western plains.

This study found that the most dramatic land-use change in SMA was the rapid expansion of the built-up area, which increased from 2727 km^2 in 2000 to 3596 km^2 in 2020. The growth of the built-up regions is closely related to China's rapid economic and urbanization development in the past two decades. The results are consistent with other China case studies [39,56–59]. However, contrary to the rapid growth of the built-up area, the cropland kept shrinking from 2000 to 2020. The overall reduction area of cropland was −1305.09 km^2, the most extensive loss among the six land-use types. These results highlight the importance of cropland protection in the SMA.

This study illustrated the usage of GEE in preparing land-use change data on a regional scale. The GEE platform enables researchers free access to large datasets on a large scale without downloading those data to their desktops. Additionally, it provides packaged algorithms for image preprocessing with relative ease, for example, random forest algorithms in this study. Furthermore, all of the processes are code-based. Therefore, extending this research to other study areas or on a denser time-series study, for example, yearly or even monthly analysis.

The study showed great ESV dynamics in the SMA during the period 2000 to 2020. The total ESVs in 2000, 2005, 2010, 2015, and 2020 were 814.04 hmCNY, 1546.82 hmCNY, 1283.78 hmCNY, 1145.76 hmCNY, and 1329.81 hmCNY, respectively. The ESV of forest land comprised the largest portion of the total ESV (from 72.65% to 77.18%), followed by water bodies (from 11.61% to 15.64%). Forest land comprised the largest proportions of land use, and water bodies are associated with the highest equivalent factors. This result highlights the importance of forest land and water bodies in SMA's ecosystem service provision. This study also found that ESVs for hydrology adjustment and ESV climate regulation are the two primary contributors of overall ESVs, since climate regulation for forests and hydrology adjustment for water bodies have the highest equivalent factors.

The ESV change analysis showed that the ESV change for forest land comprised most of the variations in the total ESV, followed by water bodies and cropland. In contrast, the water body ranked first in the perspective of the dynamic degree changes. Therefore, forest land and water bodies should be priorities in protecting ecosystem services in SMA.

4.2. Limitations

This study successfully used the GEE and a spatiotemporal adjusted value transfer method to assess land use and ESV changes in the SMA. However, some limitations and uncertainties need further investigation. First, the classification accuracy assessments indicated low grass product accuracy in 2000, 2005, 2010, 2015, and 2020, which may be caused by small sizes of reference data for grassland, and the similar spectral characteristics between cropland and grassland. Second, although we introduced a spatiotemporal correction factor to improve the equivalent factor method, some shortcomings still exist. For example, we did not consider uncertainty caused by the impact of price fluctuation or people's willingness to pay. Third, this study employed coefficient sensitivity to test the uncertainty. In this method, the CS value is employed to indicate the reliability of the results. However, we tried using ±10%, ±20%, ±30%, ±40%, and ±50% changes, and consistently obtained the same results. The results were consistent with the findings of Aschonitis et al. [60]. Therefore, future research is required for another robust sensitivity assessment method.

4.3. Contribution of This Study

First, evaluating land-use dynamics and their impact on the value of ecosystem services could provide essential information for ecosystem services-based conservation and environmental decision-making. We addressed the issue by jointly using GEE and a spatiotemporal-adjusted value transfer method, and applied it to a regional study. Our study illustrated the feasibility of this proposed method framework.

Second, the SMA is an essential economic zone in northeast China, and its ESVs have not been systematically studied. Therefore, the results can provide valuable information for future development in the SMA.

5. Conclusions

Ecosystem services provide necessary guarantees and support for human existence and good quality of life, while land-use changes could significantly alter their values. Therefore, understanding land-use dynamics and ESV changes could provide critical information for conservation and environmental decision-making. This research proposed a framework combining the GEE and a spatiotemporal-adjusted value transfer method to analyze the land-use changes and ESV dynamics of an essential economic zone in northeast China. Our main findings are as follows:

(1) forest land and cropland are the two dominant land-use types, jointly occupying 75%-89% of the total area. The built-up areas have increased rapidly, and resulted in the most significant increase (1874.43 km^2). At the same time, the cropland kept decreasing, and had the largest area reduction (1305.09 km^2), which alerts us to the need for cropland protection in the SMA.

(2) The ESV of the SMA rose substantially from 2000 (814.04 hmCNY) to 2005 (1546.82 hmCNY), then kept decreasing in 2005–2010 (−17.01%) and 2010–2015 (−10.75%), and finally increased to 1329.81 hmCNY in 2020. The ESV of forest land comprised the largest portion of the total ESV, with the percentage ranging from 72.65% to 77.18%, followed by water body, ranging from 11.61% to 15.64%. The ESV changes of forest land and water bodies are the most significant contributors to the total ESV dynamics.

(3) Fushun has the highest ecosystem service value among the five prefecture-level cities. The forest ESV of forest land comprises the largest ESV in Anshan, Fushun, Benxi, and Liaoyang, while for Shenyang, the highest ESV was from water bodies. The results highlight that forest land and water bodies should be priorities in protecting ecosystem services in SMA.

All in all, our research illustrated that the combination of GEE and the adjusted value transfer method could be helpful for the investigation of ESV changes on a regional scale. Second, the results can provide critical references for future environmental decision-making in the SMA region.

Supplementary Materials: The following are available online at https://www.mdpi.com/article/10.3390/su132212694/s1, Table S1: Landsat images used for compositing for 2000, 2005, 2010, 2015, and 2020, Table S2. Land-use type description, Table S3: Equivalent value per unit area of land-use type for ecosystem service values, Table S4: Statistical summary of land-use changes for 2000–2005, 2005–2010, 2010–2015, 2015–2020, and 2000–2020, Table S5: Total ecosystem service values by land-use type, Table S6: Ecosystem service values by ecosystem service functions, Table S7: Ecosystem service values changes by land-use type, Table S8: Ecosystem service value changes by ecosystem service functions, Table S9: Ecosystem service values of land-use type for the five prefecture-level cities, Table S10: Ecosystem service values of ecosystem service function for the five prefecture-level cities.

Author Contributions: Conceptualization, S.M.; methodology, S.M. and J.H.; validation, S.M. and J.H.; formal analysis, S.M.; writing—original draft preparation, S.M., J.H. and Y.C.; writing—review and editing, S.M. and Y.C.; visualization, S.M.All authors have read and agreed to the published version of the manuscript.

Funding: This research was supported by China's National Natural Science Foundation (No. 71801030) and the Fundamental Research Funds for the Central Universities (DUT20LAB304).

Institutional Review Board Statement: Not applicable.

Informed Consent Statement: Not applicable.

Data Availability Statement: Not applicable.

Acknowledgments: We are thankful for the data support from the National Earth System Science Data Center, National Science & Technology Infrastructure of China (http://www.geodata.cn).

Conflicts of Interest: The authors declare no conflict of interest.

References

1. Millennium Ecosystem Assessment. In *Ecosystems and Human Well-Being: Synthesis*; Island Press: Washington, DC, USA, 2005.
2. Costanza, R.; Arge, R.; Groot, R.D.; Farberk, S.; Belt, M. The value of the world's ecosystem services and natural capital. *Nature* **1997**, *387*, 253–260. [CrossRef]
3. Haines-Young, R.; Potschin, M. The links between biodiversity, ecosystem services and human well-being. *Ecosyst. Ecol. New Synthesis* **2010**, *1*, 110–139.
4. Oliveira, G.M.; Vidal, D.G.; Ferraz, M.P. Urban lifestyles and consumption patterns. In *Sustainable Cities and Communities*; Springer: Cham, Switzerland, 2020; pp. 851–860.
5. Vidal, D.G.; Barros, N.; Maia, R.L. Public and green spaces in the context of sustainable development. In *Sustainable Cities and Communities*; Encyclopedia of the UN Sustainable Development Goals; Springer: Cham, Switzerland, 2020; Volume 11, pp. 1–9.
6. Wood, S.L.; DeClerck, F. *Ecosystems and Human Well-Being in the Sustainable Development Goals*; Wiley Online Library: Hoboken, NJ, USA, 2015.
7. Peng, K.; Jiang, W.; Ling, Z.; Hou, P.; Deng, Y. Evaluating the potential impacts of land use changes on ecosystem service value under multiple scenarios in support of SDG reporting: A case study of the Wuhan urban agglomeration. *J. Clean. Prod.* **2021**, *307*, 127321. [CrossRef]
8. Vidal, D.G.; Fernandes, C.O.; Viterbo, L.M.F.; Vilaça, H.; Barros, N.; Maia, R.L. Combining an evaluation grid application to assess ecosystem services of urban green spaces and a socioeconomic spatial analysis. *Int. J. Sustain. Dev. World* **2021**, *28*, 291–302. [CrossRef]
9. Gashaw, T.; Tulu, T.; Argaw, M.; Worqlul, A.W.; Tolessa, T.; Kindu, M. Estimating the impacts of land use/land cover changes on Ecosystem Service Values: The case of the Andassa watershed in the Upper Blue Nile basin of Ethiopia. *Ecosyst. Serv.* **2018**, *31*, 219–228. [CrossRef]
10. Costanza, R.; de Groot, R.; Sutton, P.; van der Ploeg, S.; Anderson, S.J.; Kubiszewski, I.; Farber, S.; Turner, R.K. Changes in the global value of ecosystem services. *Glob. Environ. Chang.* **2014**, *26*, 152–158. [CrossRef]
11. Sutton, P.C.; Anderson, S.J.; Costanza, R.; Kubiszewski, I. The ecological economics of land degradation: Impacts on ecosystem service values. *Ecol. Econ.* **2016**, *129*, 182–192. [CrossRef]
12. Liu, Y.; Hou, X.; Li, X.; Song, B.; Wang, C. Assessing and predicting changes in ecosystem service values based on land use/cover change in the Bohai Rim coastal zone. *Ecol. Indic.* **2020**, *111*, 106004. [CrossRef]
13. Lawler, J.J.; Lewis, D.J.; Nelson, E.; Plantinga, A.J.; Polasky, S.; Withey, J.C.; Helmers, D.P.; Martinuzzi, S.; Pennington, D.; Radeloff, V.C. Projected land-use change impacts on ecosystem services in the United States. *Proc. Natl. Acad. Sci. USA* **2014**, *111*, 7492–7497. [CrossRef]
14. Wang, X.; Dong, X.; Liu, H.; Wei, H.; Fan, W.; Lu, N.; Xu, Z.; Ren, J.; Xing, K. Linking land use change, ecosystem services and human well-being: A case study of the Manas River Basin of Xinjiang, China. *Ecosyst. Serv.* **2017**, *27*, 113–123. [CrossRef]
15. Bateman, I.J.; Harwood, A.R.; Mace, G.M.; Watson, R.T.; Abson, D.J.; Andrews, B.; Binner, A.; Crowe, A.; Day, B.H.; Dugdale, S. Bringing ecosystem services into economic decision-making: Land use in the United Kingdom. *Science* **2013**, *341*, 45–50. [CrossRef] [PubMed]
16. Bai, Y.; Wong, C.P.; Jiang, B.; Hughes, A.C.; Wang, M.; Wang, Q. Developing China's Ecological Redline Policy using ecosystem services assessments for land use planning. *Nat. Commun.* **2018**, *9*, 3034. [CrossRef]
17. Wang, W.; Guo, H.; Chuai, X.; Dai, C.; Lai, L.; Zhang, M. The impact of land use change on the temporospatial variations of ecosystems services value in China and an optimized land use solution. *Environ. Sci. Policy* **2014**, *44*, 62–72. [CrossRef]
18. Boyd, J.; Banzhaf, S. What are ecosystem services? The need for standardized environmental accounting units. *Ecol. Econ.* **2007**, *63*, 616–626. [CrossRef]
19. Fu, B.; Li, Y.; Wang, Y.; Zhang, B.; Yin, S.; Zhu, H.; Xing, Z. Evaluation of ecosystem service value of riparian zone using land use data from 1986 to 2012. *Ecol. Indic.* **2016**, *69*, 873–881. [CrossRef]
20. Gorelick, N.; Hancher, M.; Dixon, M.; Ilyushchenko, S.; Thau, D.; Moore, R. Google Earth Engine: Planetary-scale geospatial analysis for everyone. *Remote Sens. Environ.* **2017**, *202*, 18–27. [CrossRef]
21. Kumar, L.; Mutanga, O. Google Earth Engine Applications Since Inception: Usage, Trends, and Potential. *Remote Sens.* **2018**, *10*, 1509. [CrossRef]
22. Zurqani, H.A.; Post, C.J.; Mikhailova, E.A.; Schlautman, M.A.; Sharp, J.L. Geospatial analysis of land use change in the Savannah River Basin using Google Earth Engine. *Int. J. Appl. Earth Obs.* **2018**, *69*, 175–185. [CrossRef]
23. Ji, Q.; Liang, W.; Fu, B.; Zhang, W.; Yan, J.; Lü, Y.; Yue, C.; Jin, Z.; Lan, Z.; Li, S.; et al. Mapping Land Use/Cover Dynamics of the Yellow River Basin from 1986 to 2018 Supported by Google Earth Engine. *Remote Sens.* **2021**, *13*, 1299. [CrossRef]
24. Mutanga, O.; Kumar, L. Google Earth Engine Applications. *Remote Sens.* **2019**, *11*, 591. [CrossRef]
25. Tsai, Y.; Stow, D.; Chen, H.; Lewison, R.; An, L.; Shi, L. Mapping Vegetation and Land Use Types in Fanjingshan National Nature Reserve Using Google Earth Engine. *Remote Sens.* **2018**, *10*, 927. [CrossRef]
26. Robinson, N.; Allred, B.; Jones, M.; Moreno, A.; Kimball, J.; Naugle, D.; Erickson, T.; Richardson, A. A Dynamic Landsat Derived Normalized Difference Vegetation Index (NDVI) Product for the Conterminous United States. *Remote Sens.* **2017**, *9*, 863. [CrossRef]

27. He, M.; Kimball, J.; Maneta, M.; Maxwell, B.; Moreno, A.; Beguería, S.; Wu, X. Regional Crop Gross Primary Productivity and Yield Estimation Using Fused Landsat-MODIS Data. *Remote Sens.* **2018**, *10*, 372. [CrossRef]
28. Aguilar, R.; Zurita-Milla, R.; Izquierdo-Verdiguier, E.; A De By, R. A Cloud-Based Multi-Temporal Ensemble Classifier to Map Smallholder Farming Systems. *Remote Sens.* **2018**, *10*, 729. [CrossRef]
29. Schneider, A. Monitoring land cover change in urban and peri-urban areas using dense time stacks of Landsat satellite data and a data mining approach. *Remote Sens. Environ.* **2012**, *124*, 689–704. [CrossRef]
30. E Nyland, K.; E Gunn, G.; I Shiklomanov, N.; N Engstrom, R.; A Streletskiy, D. Land Cover Change in the Lower Yenisei River Using Dense Stacking of Landsat Imagery in Google Earth Engine. *Remote Sens.* **2018**, *10*, 1226. [CrossRef]
31. Liu, C.; Li, W.; Zhu, G.; Zhou, H.; Yan, H.; Xue, P. Land Use/Land Cover Changes and Their Driving Factors in the Northeastern Tibetan Plateau Based on Geographical Detectors and Google Earth Engine: A Case Study in Gannan Prefecture. *Remote Sens.* **2020**, *12*, 3139. [CrossRef]
32. Xie, G.; Zhang, C.; Zhen, L.; Zhang, L. Dynamic changes in the value of China's ecosystem services. *Ecosyst. Serv.* **2017**, *26*, 146–154. [CrossRef]
33. Tolessa, T.; Senbeta, F.; Kidane, M. The impact of land use/land cover change on ecosystem services in the central highlands of Ethiopia. *Ecosyst. Serv.* **2017**, *23*, 47–54. [CrossRef]
34. Sannigrahi, S.; Bhatt, S.; Rahmat, S.; Paul, S.K.; Sen, S. Estimating global ecosystem service values and its response to land surface dynamics during 1995–2015. *J. Environ. Manag.* **2018**, *223*, 115–131. [CrossRef]
35. Xie, G.D.; Zhen, L.; Chun-Xia, L.U.; Xiao, Y.; Chen, C. Expert Knowledge Based Valuation Method of Ecosystem Services in China. *J. Nat. Resour.* **2008**, *23*, 911–919. (In Chinese)
36. Xie, G.D.; Zhang, C.X.; Zhang, L.M.; Chen, W.H.; Li, S.M. Improvement of the Evaluation Method for Ecosystem Service Value Based on Per Unit Area. *J. Nat. Resour.* **2015**, *30*, 1243. (In Chinese)
37. Ye, Y.; Bryan, B.A.; Zhang, J.; Connor, J.D.; Chen, L.; Qin, Z.; He, M. Changes in land-use and ecosystem services in the Guangzhou-Foshan Metropolitan Area, China from 1990 to 2010: Implications for sustainability under rapid urbanization. *Ecol. Indic.* **2018**, *93*, 930–941. [CrossRef]
38. Song, W.; Deng, X. Land-use/land-cover change and ecosystem service provision in China. *Sci. Total Environ.* **2017**, *576*, 705–719. [CrossRef] [PubMed]
39. Ye, Y.; Zhang, J.; Wang, T.; Bai, H.; Wang, X.; Zhao, W. Changes in Land-Use and Ecosystem Service Value in Guangdong Province, Southern China, from 1990 to 2018. *Land* **2021**, *10*, 426. [CrossRef]
40. Song, W.; Deng, X.; Yuan, Y.; Wang, Z.; Li, Z. Impacts of land-use change on valued ecosystem service in rapidly urbanized North China Plain. *Ecol. Model* **2015**, *318*, 245–253. [CrossRef]
41. Sannigrahi, S.; Chakraborti, S.; Joshi, P.K.; Keesstra, S.; Sen, S.; Paul, S.K.; Kreuter, U.; Sutton, P.C.; Jha, S.; Dang, K.B. Ecosystem service value assessment of a natural reserve region for strengthening protection and conservation. *J. Environ. Manag.* **2019**, *244*, 208–227. [CrossRef]
42. Statistics Bureau of Liaoning Province. *Liaoning Statistical Yearbook 2001*; China Statistics Press: Beijing, China, 2001.
43. Statistics Bureau of Liaoning Province. *Liaoning Statistical Yearbook 2020*; China Statistics Press: Beijing, China, 2020.
44. Wingate, V.; Phinn, S.; Kuhn, N.; Bloemertz, L.; Dhanjal-Adams, K. Mapping Decadal Land Cover Changes in the Woodlands of North Eastern Namibia from 1975 to 2014 Using the Landsat Satellite Archived Data. *Remote Sens.* **2016**, *8*, 681. [CrossRef]
45. Coulter, L.L.; Stow, D.A.; Tsai, Y.; Ibanez, N.; Shih, H.; Kerr, A.; Benza, M.; Weeks, J.R.; Mensah, F. Classification and assessment of land cover and land use change in southern Ghana using dense stacks of Landsat 7 ETM+ imagery. *Remote Sens. Environ.* **2016**, *184*, 396–409. [CrossRef]
46. Tucker, C.J. Red and photographic infrared linear combinations for monitoring vegetation. *Remote Sens. Environ.* **1979**, *8*, 127–150. [CrossRef]
47. Xu, H. Extraction of Urban Built-up Land Features from Landsat Imagery Using a Thematicoriented Index Combination Technique. *Photogramm. Eng. Remote Sens.* **2007**, *73*, 1381–1391. [CrossRef]
48. Xu, X.; Liu, J.; Zhang, S.; Li, R.; Yan, C.; Wu, S. (Eds.) *China Multi-Period Land Use and Land Cover Remote Sensing Monitoring Data Set (CNLUCC)*; Data Registration and Publishing System of the Resource and Environmental Science Data Center of the Chinese Academy of Sciences; Resource and Environmental Science Data Center: Beijing, China, 2018. Available online: http://www.resdc.cn/DOI (accessed on 8 June 2021).
49. Tian, S.; Zhang, X.; Tian, J.; Sun, Q. Random Forest Classification of Wetland Landcovers from Multi-Sensor Data in the Arid Region of Xinjiang, China. *Remote Sens.* **2016**, *8*, 954. [CrossRef]
50. Schmidt, M.; Pringle, M.; Devadas, R.; Denham, R.; Tindall, D. A Framework for Large-Area Mapping of Past and Present Cropping Activity Using Seasonal Landsat Images and Time Series Metrics. *Remote Sens.* **2016**, *8*, 312. [CrossRef]
51. Congalton, R.G.; Green, K. *Assessing the Accuracy of Remotely Sensed Data: Principles and Practices*; CRC Press: Boca Raton, FL, USA, 2019.
52. Yoshida, A.; Chanhda, H.; Ye, Y.; Liang, Y. Ecosystem service values and land use change in the opium poppy cultivation region in Northern Part of Lao PDR. *Acta Ecol. Sin.* **2010**, *30*, 56–61. [CrossRef]
53. Kreuter, U.P.; Harris, H.G.; Matlock, M.D.; Lacey, R.E. Change in ecosystem service values in the San Antonio area, Texas. *Ecol. Econ.* **2001**, *39*, 333–346. [CrossRef]

54. Kindu, M.; Schneider, T.; Teketay, D.; Knoke, T. Changes of ecosystem service values in response to land use/land cover dynamics in Munessa–Shashemene landscape of the Ethiopian highlands. *Sci. Total Environ.* **2016**, *547*, 137–147. [CrossRef]
55. Liu, Y.; Li, J.; Zhang, H. An ecosystem service valuation of land use change in Taiyuan City, China. *Ecol. Model* **2012**, *225*, 127–132. [CrossRef]
56. Wang, X.; Yan, F.; Zeng, Y.; Chen, M.; Su, F.; Cui, Y. Changes in Ecosystems and Ecosystem Services in the Guangdong-Hong Kong-Macao Greater Bay Area since the Reform and Opening Up in China. *Remote Sens.* **2021**, *13*, 1611. [CrossRef]
57. Xiao, R.; Lin, M.; Fei, X.; Li, Y.; Zhang, Z.; Meng, Q. Exploring the interactive coercing relationship between urbanization and ecosystem service value in the Shanghai–Hangzhou Bay Metropolitan Region. *J. Clean. Prod.* **2020**, *253*, 119803. [CrossRef]
58. Li, Y.; Zhan, J.; Liu, Y.; Zhang, F.; Zhang, M. Response of ecosystem services to land use and cover change: A case study in Chengdu City. *Resour. Conserv. Recycl.* **2018**, *132*, 291–300. [CrossRef]
59. Li, Y.; Feng, Y.; Guo, X.; Peng, F. Changes in coastal city ecosystem service values based on land use—A case study of Yingkou, China. *Land Use Policy* **2017**, *65*, 287–293. [CrossRef]
60. Aschonitis, V.G.; Gaglio, M.; Castaldelli, G.; Fano, E.A. Criticism on elasticity-sensitivity coefficient for assessing the robustness and sensitivity of ecosystem services values. *Ecosyst. Serv.* **2016**, *20*, 66–68. [CrossRef]